

Implementation of a Low Order Mimetic Elements in freefem++

D. DALAL^{*}, F. HECHT[†], and O. PIRONNEAU[†]

Received May 30, 2012

Communicated by Yu. A. Kuznetsov

Received in revised form July 1, 2012

Abstract — This paper describes an implementation in freefem++ of a mimetic scheme due to Yu. Kuznetsov. This is done by a minor modification of the program which implements the totally discontinuous Raviart-Thomas element RT0 because both elements have similar degrees of freedom. The method is tested in combination with characteristic-Galerkin unwinding on the rotating hill problem.

Keywords: Mimetic Element, Finite Element, characteristic-Galerkin, convection diffusion equation, partial differential equation. Black oil problem

1. Introduction

A general framework for mimetic schemes has been built by F. Brezzi et al (yet to be published). The original idea seems to be Shashkov's (see [3]); it was used and enlarged to a Finite Element context by Brezzi and Lipnikov[2] and many others since then.

The upside of mimetic methods is that it allows any polygon in a tessaliation of the domain of the PDE, not just triangles and quadrangles; also, an element inner edge may be shared in part by several elements on the other side.

The downside of mimetics is the difficulty of their computer implementation. Aware of this problem, Yu. Kuznetsov had been working down-up on an alternative, with success for porous media flows in 2D and 3D, much easier to implement.

It turns out that for piecewise constant approximations both methods agree in the special case where the quadrangles are divided into 4 equal elements (Figure 1); we give here similar division for triangles.

Eager to try these new methods the authors thought out a way to implement them in freefem++. This article is the story of their implementation and a report on performance for the general convection-diffusion equation.

^{*}Dept. of Mathematics, IIT-Guwahati, Guwahati 781039, India

[†]LJLL-UPMC (Paris VI) Boite 187, Place Jussieu F-75252 Paris

This work was supported by "ANR Cosinus" and "Sciences Mathématiques de Paris".

The presentation of the finite element method follows the line of a private lecture by Yu. Kuznetsov but more details are available in [6].

2. Problem Statement and Discretization

For simplicity consider the Laplace equation written as a first order system (generalization to Darcy's law and time dependent convection-diffusion equations are in [7],[5], [6] and below):

$$u + \nabla p = 0, \quad \nabla \cdot u = f, \quad \text{in } \Omega \quad + \quad \text{b.c. on } \Gamma = \partial\Omega. \quad (2.1)$$

The domain Ω is covered by a set of non-overlapping elements E . The edges of E are called generically S . Note that for any integrable scalar or vector-valued q and any vector-valued v with integrable normal component,

$$q_S := \frac{1}{|S|} \int_S q(x) d\gamma(x), \quad q_E := \frac{1}{|E|} \int_E q(x) dx, \quad v_S^n := \frac{1}{|S|} \int_S v(x) \cdot n(x) d\gamma(x). \quad (2.2)$$

are piecewise constant quantities.

Proposition 2.1. *Let V_S^E be the space of vector-valued functions $v : E \rightarrow \mathbf{R}^2$ such that $\nabla \cdot v$ is constant on E and $v \cdot n$ is constant on each edge $S \in \partial E$; then (2.1) implies*

$$\int_E u \cdot v dx + \sum_{S \in \partial E} (p_S - p_E) v_S^n |S| = 0, \quad \forall v \in V_S^E, \quad \forall E \quad (2.3)$$

$$\sum_{S \in \partial E} u_S^n |S| = |E| f_E, \quad \forall E. \quad (2.4)$$

Proof

The second equation of (2.1) integrated on E gives (2.4). To derive (2.3) let us multiply the first equation of (2.1) by $v \in V_S^E$ and integrate the second term by parts:

$$\int_E u \cdot v dx + \int_{\partial E} p v \cdot n d\gamma - \int_E p \nabla \cdot v dx = 0. \quad (2.5)$$

By making use of the fact that $\nabla \cdot v$ is constant we can write that

$$\int_E p \nabla \cdot v dx = p_E |E| \nabla \cdot v = p_E \int_E \nabla \cdot v dx = p_E \int_{\partial E} v \cdot n d\gamma = p_E \sum_{S \in \partial E} v_S^n |S|. \quad (2.6)$$

This proves (2.3)(2.4).

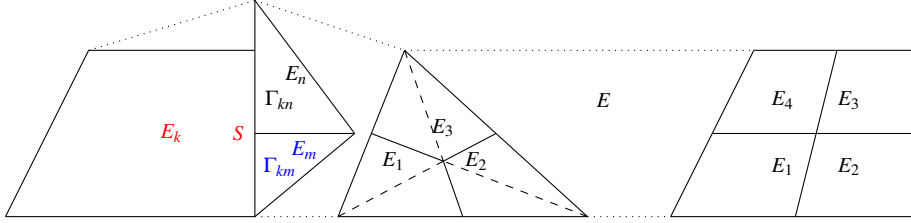


Figure 1. The mesh is made of a union of polygons. A portion of the mesh is shown highlighting 5 elements and the fact that the edges of adjacent elements do not need to match. Notations for elements and edges are shown on the left with $\Gamma_{km} := E_k \cap E_m$. Center and right: each polygon is subdivided so that each sub-element shares two edges with its mother element; this is shown in the center on a triangle E with its 3 quadrilateral sub-elements $\{E_i\}_1^3$ of equal size and on the right on a quadrangle E with its 4 sub-elements of equal size $\{E_i\}_1^4$.

2.1. Discrete Approximation equivalent to Shashkov's Mimetic Scheme

The notations are explained in Figure 1. Note that a constant vector w can be reconstructed from two fluxes on non parallel edges S_1, S_2 , $w_{S_i}^n := \mathbf{w} \cdot \mathbf{n}^i$, $i = 1, 2$ where \mathbf{n}^i is the outer normal to the edge S_i :

$$\mathbf{w} = \mathbf{n}^1 \frac{w_{S_1}^n - w_{S_2}^n n_1 \cdot n_2}{1 - (n_1 \cdot n_2)^2} + \mathbf{n}^2 \frac{w_{S_2}^n - w_{S_1}^n n_1 \cdot n_2}{1 - (n_1 \cdot n_2)^2}. \quad (2.7)$$

Now, in (2.3) and (2.4) everything is discrete except the first term. So let us reconstruct u in E from its fluxes on ∂E . Following [6] the reconstruction is piecewise constant but discontinuous:

- Each **triangle** E is divided into 3 quadrilaterals of equal size by the medians as shown in Figure 1. The number of sub-elements is $d_E = 3$.
- Each **quadrilateral** element E is divided in 4 quadrilaterals of equal size by joining the mid-points of two facing edges as in Figure 1. Here $d_E = 4$.
- More complex **polygons** are divided into sub-elements so that each of them has 2 (and only 2) common boundaries with ∂E .

With u_{E_i} reconstructed by (2.7) from the fluxes on the two non internal edges of E_i , the following approximation is used

$$\int_E u \cdot v dx \approx \sum_1^{d_E} u_{E_i} \cdot v_{E_i} |E_i|. \quad (2.8)$$

Two cases can be considered:

- The totally discontinuous case in which the flux v_S^n seen from E is different from the flux on S but seen from the adjacent element E' .

- The semi-continuous case in which v_S^n is the same seen from E and E' .

Definition 2.1. *In the semi-continuous case the degrees of freedom of the finite element are p_E, u_S^n and p_E, p_S, u_S^n in the totally discontinuous case*

In the totally discontinuous a weak continuity at the edges must be imposed by

$$\sum_E \sum_{S \in \partial E} \int_S q_S u_S^n d\gamma(x) = 0, \quad \forall q_S. \quad (2.9)$$

The numerical scheme is made of (2.3)(2.4) in the semi-continuous case and (2.3)(2.4) (2.9) in the totally discontinuous case, both using (2.8).

Remark 2.1. Suppose we have n quadrilaterals and m triangles then there are $M = n + m$ elements and $N = 4n + 3m$ edges S ; so the number of degrees of freedom is $2N + M$. Because V_S^E is constructed from the fluxes at the edges, $\dim V_S^E = 4$ for quadrilaterals and 3 for triangles; so the number of equations in (2.3) is $4n + 3m$ and M in (2.4). As the number of equations in (2.9) is N the total number of equations $4n + 3m + M + N = M + 2N$ is equal to the number of unknowns. The scheme is proved to be well posed in [6] for example.

Remark 2.2. If there are quadrilaterals only, the scheme is exactly Shashkov's mimetic scheme [3][2]. The convergence analysis for the scheme above is available in [8]

Remark 2.3. There are many mimetic finite difference schemes, usually only distinct by the numerical quadrature applied to the first term in the first equation of (2.3). Recently, it has been shown in [9] that the classical mixed finite element methods also fall into the mimetic finite difference family on arbitrary polygonal/polyhedral meshes when some local problems are solved on the triangular submesh mesh of each polygonal. Such an approach has the particular advantage that no approximation/numerical quadrature is needed and the precision of simplicial mixed finite elements is fully maintained, while the implementation is straightforward from an existing mixed finite element code.

3. Extension to time dependent problems with convection

With $a \in L^\infty(\mathbf{R}^d \times (0, T))$, $A \in L^\infty(\mathbf{R}^{d \times d} \times (0, T))$, the convection-diffusion equation

$$\partial_t p + a \cdot \nabla p - \nabla \cdot (A \nabla p) = f + b.c. \quad \text{and } u(\cdot, 0) \text{ given}$$

is rewritten in mixed form with $D = A^{-1}$ as

$$\partial_t p + a \cdot \nabla p + \nabla \cdot u = f, \quad Du + \nabla p = 0, \quad +b.c... \quad (3.1)$$

It can be discretized in time by

$$\frac{1}{\delta t} p^m + \nabla \cdot u^m = \tilde{f}^m := f(x) + \frac{1}{\delta t} p^{m-1} (x - a^{m-\frac{1}{2}}(x) \delta t), \quad Du^m + \nabla p^m = 0. \quad (3.2)$$

With the totally discontinuous element, a spatial discretization like (2.3) (2.4) (2.7) gives the following system:

Definition 3.1. For the totally discontinuous method, the discrete problem is

$$\begin{aligned} \sum_E \sum_1^{d_E} v_{E_i}^T D u_{E_i} |E_i| + \sum_E \sum_{S \in \partial E} (p_S - p_E) v_S^n |S| &= 0, \quad \forall v \in V_S^E, \\ \sum_E \frac{|E|}{\delta t} p_E q_E + \sum_E \sum_{S \in \partial E} u_S^n q_E |S| &= \sum_E |E| \tilde{f}_E^m q_E, \quad \forall q_E \in Q_E, \\ \sum_E \sum_{S \in \partial E} q_S u_S^n |S| &= 0, \quad \forall q_S \in Q_S. \end{aligned} \quad (3.3)$$

where V_S^E is the finite element space of vector-valued functions defined by their fluxes on the edges seen from each element (two fluxes), Q_S is the space of affine functions defined by their fluxes on the edges and Q_E is the space of P^0 functions on the elements.

In the case of the semi-continuous element, V_S^E is replaced by V_S the same space but with fluxes equal on the left and right of each inner edge S of the mesh; in that case the third equation is not needed.

4. Implementation in freefem++

The Raviart-Thomas element RT0 and the totally discontinuous RT0 were already in freefem++, which, by the way, handles only triangles. By dividing the triangles in 3 sub-element, as shown in Figure 1, the logic of the element is the same as RT0 and the interpolation inside the element is similar.

Indeed the hat function φ^j associated with the edge opposite vertex q^j is proportional to $\vec{x} - \vec{q}^j$ and the value of this function at the one of the two other vertices q^i is exactly equal to the value given by (2.7) when $w_S^n = \delta_{ij}$. So instead of assigning φ^i to the opposite edge, one assign it to the quadrangle which contains q^i ; this amounts to 3 extra lines of C++ code only. As the sub-elements have the same area, the only thing needed is to make sure that integrals are computed by a quadrature formula which uses the vertices for quadrature points (see the keyword `qf1pT1ump` below), namely mass lumping.

The program in Figure 2 shows the script to solve $-\Delta p = 1$, $p|_\Gamma = 0$ with $\Omega = (0, 1)^2$. An error plot on fig. 2 for this problem shows that the method is indeed of order one with respect to the mesh size. A problem with discontinuous coefficient

and analytical answer was also tested and similarly perfect order one L^2 error was observed.

To test the full convection-diffusion equation we solved the rotating hill problem in the unit square discretized on a 40×40 uniform mesh with $\delta t = 0.1$,

$$p(x, y, 0) = e^{-100*((x-0.75)^2+(y-0.75)^2)}, \quad \mathbf{v} = 0.001 \text{ and} \\ a = (y - \frac{1}{2}, \frac{1}{2} - x), A_{11} = \mathbf{v} * (1 + (x < \frac{1}{2})), A_{22} = \mathbf{v}, A_{12} = -\frac{\mathbf{v}}{2}, A_{21} = 0. \quad (4.1)$$

The solver at each time step is programmed by (pt is $p^m|_T$ and pto is $p^{m-1}|_T$)

```
problem kuz([pe,pt,u1,u2],[qe,qt,v1,v2])
= int2d(th,qft=qf1pTlump)( [u1,u2]'*[[D11,D12],[D21,D22]]*[v1,v2] )
+ int2d(th)(pt*qt/dt)
+ intalldges(th)( (pe-pt)*(v1*N.x+v2*N.y) + (u1*N.x+u2*N.y)*(qt+qe/2) )
- int2d(th)((f + ptoId(x-a1*dt,y-a2*dt)/dt)*qt ) + on(1,2,3,4,pe=0);
```

After half a turn the hill has decreased due to diffusion as shown in Figure 2.

4.1. Performance on the black oil problem

To enhance the oil recovery, an hydrocarbon solvent or water is injected by a well to push the oil into the recovering well. When the fluids are miscible and incompressible, the replacement may be governed by the following set of equations (see [1]),

$$\nabla \cdot \mathbf{u} = 0, \quad \mathbf{u} = -\frac{k}{\mu(c)} \nabla p, \quad (4.2)$$

$$\varphi \frac{\partial c}{\partial t} + \nabla \cdot (uc) = D \nabla^2 c, \quad (4.3)$$

where the domain is considered to be a unit square, \mathbf{u} is the velocity of fluid, p is fluid pressure, c the volume fraction of solvent, φ the porosity, k the permeability of the medium, D is a constant diffusion coefficient and μ is the viscosity of the homogeneous mixture of oil and solvent which is a function of c and given as (due to Koval [4]),

$$\mu(c) = \left[\mu_s^{-1/4} c + \mu_o^{-1/4} (1 - c) + \varepsilon \right]^{-4}, \quad (4.4)$$

μ_s and μ_o represent viscosities of solvent and oil respectively and ε is a small number to insure that μ is always strictly positive.

The non-dimensional form of the governing equations are written as,

$$\nabla \cdot \mathbf{u} = 0, \quad \nabla p = - \left[c + (1 - c) M^{-1/4} \right]^{-4} \mathbf{u}, \quad (4.5)$$

$$\frac{\partial c}{\partial t} + \nabla \cdot (uc) = Pe \nabla^2 c, \quad (4.6)$$

```

load "Kuz"
load "splitmesh6"
int n=40, LL=1;
mesh th = square(2*n,2*n,[x,y*LL]);
mesh th6 = splitmesh6(th);
fespace KT0h(th,KT0dc);
KT0h [u1,u2],[v1,v2];

fespace PEh(th,P0edge);
PEh pe,qe;

fespace PTh(th,P0);
PTh pt,qt, f=1;

real D11=1,D22=1,D12=0,D21=0;
problem kuz([pe,pt,u1,u2],[qe,qt,v1,v2])
  = int2d(th,qft=qf1pTlump)(
    [u1,u2]'*[[D11,D12],[D21,D22]]*[v1,v2]
  + intalldges(th)((pe-pt)*(v1*N.x+v2*N.y)
  + (u1*N.x+u2*N.y)*(qt+qe/2)
  ) - int2d(th)(f*qt) + on(1,2,3,4,pe=0);
kuz;
plot([u1,u2], wait=1);
plot(pt, dim=3, fill=true);

```

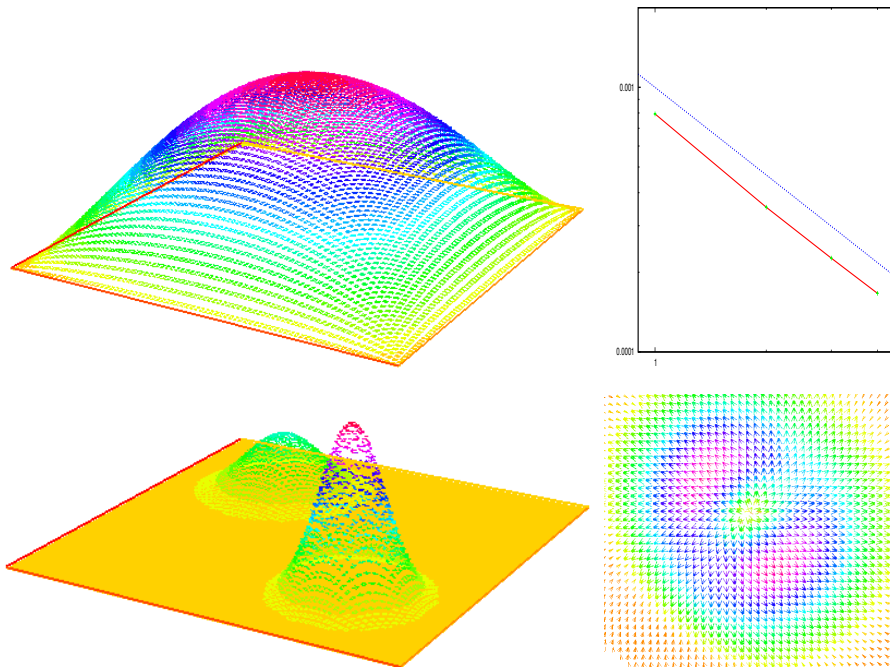


Figure 2. Freefem script (top) and results (middle) on $-\Delta p = 1$, $p|_{\Gamma} = 0$ by the totally discontinuous mimetic element. In the middle on the left the log-log error plot has a slope equal to -1.1. Bottom: the rotating hill at $t = 0$ and at $t = 3.1$. On the right a zoom around the tip of the hill shows the velocity field at final time.

where reservoir length L is the length scale, $\phi L/U$ the time scale, U is representative flux of fluid, pressure is made non-dimensional by the term $LU\mu_s/k$, Péclet number $Pe = UL/D$ and the mobility ratio $M = \mu_o/\mu_s$.

The boundary conditions are taken as,

$$c = 1, \quad p = 1, \text{ at the injection well and } p = 0, \text{ at the recovery well} \quad (4.7)$$

Normal derivatives of c and p are assumed to be zero on the remaining boundaries; in the freefem script these boundary conditions are applied by adding to the definitions of the PDE of u, p

$$+ \text{int1d}(\text{th}, \text{r1}) ([v1, v2]' * [N.x, N.y] * 1) + \text{on}(s1, s2, s3, s4, u1=0, u2=0)$$

where r1 is the injecting well and $s1, s2, s3, s4$ are the sides of the square domain. Notice that even though $u1 = u2 = 0$ is specified, freefem will automatically select only the normal component and enforce $\mathbf{u} \cdot \mathbf{n} = \mathbf{0}$. Similarly for the PDE for c and its gradient $\mathbf{a} = \nabla c$ is

```
problem concentration([c,a1,a2],[wt,b1,b2])
= int2d(th,qft=qf1pTlump)( [a1,a2]'*[b1,b2] / Pe )
+ intalldges(th)(-c*(b1*N.x+b2*N.y) + (a1*N.x+a2*N.y)*wt)
+ int2d(th)(c*wt/dt)
- int2d(th)( convect([u1,u2],-dt,c_old)*wt/dt)
+ on(r1,s1,s2,s3,s4,a1=0,a2=0) + on(r1,c=1)
```

First we made a test to assert the precision of the method when the porosity is highly discontinuous. So we solved in the unit square

$$\nabla \cdot \mathbf{u} = 0, \quad \mathbf{u} = -K \nabla p, \quad p(0,y) = 1, \quad p(1,y) = 0, \quad \frac{\partial p}{\partial x} = 0 \text{ at } y = 0, 1 \quad (4.8)$$

with $K = K_0 + (K_1 - K_0)\mathbf{1}_{x>0.5}$ with very large values of K_1/K_0 . The L^2 error plot on p shown on figure 3 does not depend on K_1/K_0 in the range $[10^6, 10^{12}]$ and shows optimal order 1.

Miscible viscous fingering generally occur at high value of Péclet number Pe [4],[1]. For the numerical simulation M and Pe are taken as $M = 5$ and $Pe = 3000$ respectively and $\varepsilon = 0.1$. Calculations are performed on a mesh with 10760 vertices and 21138 triangles with a time step of 0.02. Results are shown on fig. 4 at $T=3$. A comparison is made with the P^1 -element for both equations; the computing time is twice shorter with the later which however is known to be less stable on these problems in general (but stable here). Because fingering is an unstable phenomenon one cannot expect that both methods would give the same results. Nevertheless the results are of similar nature and time scale.

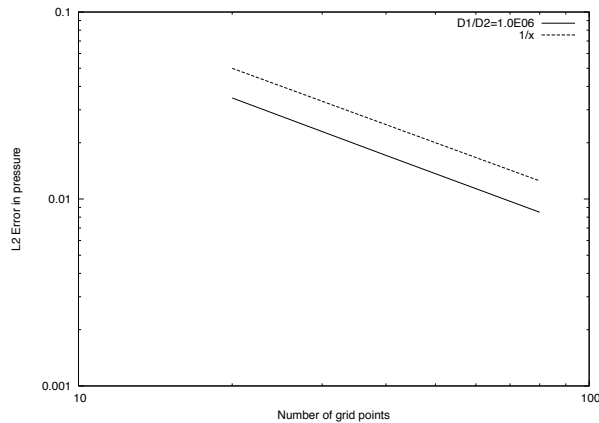


Figure 3. The L^2 error plot on p solution (4.8) for 4 uniform meshes from 40×40 to 160×160 and $K_1/K_0 = 10^9$

Conclusion

We have shown that it is easy to implement the mimetic methods in freefem++, at least in the case of low order polynomials. However freefem++ is limited to triangles only, a restriction that kills much of the qualities of mimetic approximations. In the future we plan to extend this work in two directions:

1. Create an element which can be divided by a line representing a fault and on which the permeability can take two different values and use mimetics on both parts.
2. Allow the user to cluster triangles and define his mimetic approximation on these clusters.

Acknowledgement

We thank the reviewer for suggesting the "cluster idea" and for drawing our attention to [9].

References

1. R.J.S. BOOTH, *On the growth of the mixing zone in miscible viscous fingering*. *J.Fluid Mech.* **655**, (2010) 527-539 .
2. F. BREZZI AND K. LIPNIKOV AND V. SIMONCINI, *A family of mimetic finite difference methods on polygonal and polyhedral meshes* , *Mathematical Models and Methods in Applied Sciences* Vol. 15, No. 10 (2005) 1533-1551.
3. J. HYMAN, M. SHASHKOV AND S. STEINBERG, *The numerical solution of diffusion problems in strongly heterogeneous non-isotropic materials*, *J. Comput. Phys.* 132 (1997) 130-148.

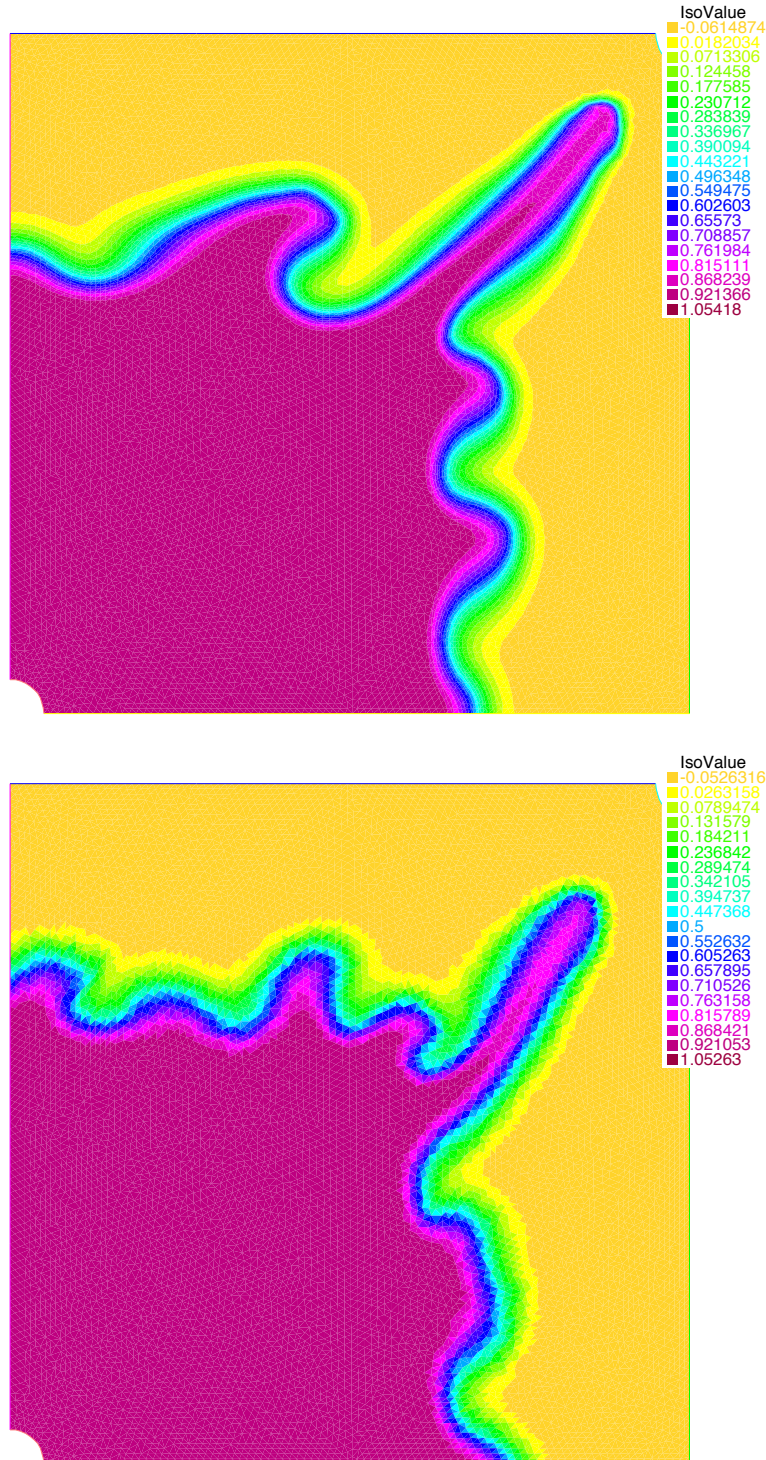


Figure 4. Fingering at $T=3$ by classic P1 FEM (left) and with the new mimetic element (right)

-
4. J.E. KOVAL, *A method for predicting the performance of unstable miscible displacement in heterogeneous media. SPE J.* **450**, (1963) 145-154.
 5. YU. KUZNETSOV, *Mixed finite element method for diffusion equations on polygonal meshes with mixed cells*, J. Numer. Math., Vol. 14, No. 4, pp. 305-315 (2006)
 6. YU. KUZNETSOV, *Approximations with piecewise constant fluxes for diffusion equations*, J. Numer. Math. 10 (4) pp– 2012.
 7. YU. KUZNETSOV AND S. REPIN, *New mixed finite element method on polygonal and polyhedral meshes*, Russ. J. Numer. Anal. Math. Modelling 18, No. 3, 261-278 (2003).
 8. YU. KUZNETSOV AND S. REPIN, *Convergence analysis and error estimates for mixed finite element on distorted meshes* J. Numer. Math, Vol. 13, No 1., pp31-51 (2005).
 9. M. VOHRALIK, AND B. I. WOHLMUTH. *Mixed finite element methods: implementation with one unknown per element, local flux expressions, positivity, polygonal meshes, and relations to other methods.* HAL Preprint 00497394, submitted for publication, 2010.